Photoluminescence measurements of tensile-strained GaAs/$In_{0.07}Al_{0.93}As$ quantum wells

C. N. Yeh[a] and L. E. McNeil
Department of Physics and Astronomy, University of North Carolina at Chapel Hill, Chapel Hill, North Carolina 27599-3255

T. Daniels-Race
Department of Electrical Engineering, Duke University, Durham, North Carolina 27708-0291

L. J. Blue
Department of Physics, Box 90305, Duke University, Durham, North Carolina 27708-0305

(Received 6 November 1995; accepted for publication 4 December 1995)

GaAs/$In_{0.07}Al_{0.93}As$ tensile-strained quantum wells were grown on [001] GaAs substrates using molecular-beam epitaxy. The incorporation of tensile strain is made possible by preparing a 1-μm-thick $In_{0.07}Al_{0.93}As$ relaxed buffer which is followed by the growth of quantum wells. The strain of the GaAs was measured using Raman spectroscopy and photoluminescence. The photoluminescence measurements from wells ranging in thickness from 25 to 100 Å reveal that the observed optical transition originates from the electron–light hole recombination for a 100 Å well and from the electron–heavy hole recombination if the well thickness is less than 40 Å. Therefore, a thick Al-rich $In_xAl_{1-x}As$ relaxed buffer on the GaAs substrate can be used to engineer the relative energy position of the light and heavy holes for GaAs-based quantum wells. © *1996 American Institute of Physics.* [S0021-8979(96)01906-X]

INTRODUCTION

Strained-layer heterostructures offer advantages over lattice-matched heterostructures in the choice of materials and performance of optoelectronic devices. Detailed studies of semiconductor quantum-well lasers made of $In_xGa_{1-x}As$/AlGaAs[1] and $In_xGa_{1-x}As$/InGaAsP[2] have demonstrated that the incorporation of compressive strain into the quantum wells can provide benefits of lower threshold current density and higher gain. This is because the compressive strain reduces the in-plane (xy) effective mass of the top valence band $|3/2,\pm 3/2\rangle$ (heavy hole) and consequently the lower density of states in the hole band results in a smaller current density being needed to achieve the population inversion condition.[3] For tensile-strained quantum wells, the strain raises the energy of $|3/2,\pm 1/2\rangle$ (light hole) valence band. Theoretical calculations[4,5] indicate that the in-plane (xy) effective mass of the tensile-strained light-hole (lh) valence band is larger than that of the compressive-strained heavy hole valence band. However, it has been demonstrated[6–8] that incorporation of tensile strain can also reduce the threshold current density of the quantum-well laser if a larger strain or thicker well is employed.

The top valence band of a compressive-strained quantum well is always the heavy hole (hh) no matter what the well thickness is. This is because the compressive strain raises the energy of the hh, which has a larger effective mass than that of the lh in the [001] direction, and the confinement effect splits the energy separation between the hh and lh further in a thinner well. For the tensile-strained quantum well, the top valence band is the lh in a wider well due to the strain effect. However, the hh can be at the top of the valence band if the well is thin enough that the difference in confinement energies of the hh and the lh exceeds their strain-induced splitting. Due to the nature of the hh and the lh, the photon polarization of the in-plane optical transition, for which the photon propagates along the quantum-well plane, is different for the e–hh and e–lh transitions. Only the TE polarization (the electric field perpendicular to the [001] direction) is allowed for the e–hh transition, while both TE and TM modes are allowed for the e–lh transition.[9] In essence, the polarization of the in-plane interband optical transition of an unstrained or compressive-strained quantum well is anisotropic.[10–12] Polarization-insensitive devices utilizing tensile-strained quantum wells have been reported, including an electroabsorption modulator,[13,14] a dual-polarization laser diode,[15] and a semiconductor photodetector.[6] Most of the work in tensile-strained quantum wells is based on InGaAs/InGaAsP and InGaAlP/InGaP[16,17] quantum wells. The tensile-strained GaAs quantum well has been less studied.[18,19] For the realization of a tensile-strained GaAs quantum well grown on a GaAs substrate, it is necessary to prepare a thick, relaxed, and high band-gap ternary alloy, such as Al-rich $In_xAl_{1-x}As$, with a larger lattice constant to strain the GaAs quantum well. In this work, we report photoluminescence (PL) measurements of tensile-strained GaAs/$In_{0.07}Al_{0.93}As$ quantum wells. The data are analyzed using the four-band $\mathbf{k}\cdot\mathbf{p}$ theory to reveal the origins of PL peaks. The strain of the GaAs is also determined from the analysis and compared with the Raman measurement.

EXPERIMENT

The samples studied in this work were grown on [001]-oriented GaAs substrates using molecular-beam epitaxy. The growth rate was one monolayer/s for GaAs quantum wells and 0.7 monolayer/s for $In_{0.07}Al_{0.93}As$. The substrate tem-

[a]Electronic mail: yeh@physics.unc.edu

 0021-8979/96/79(6)/3192/4/$10.00

TABLE I. Tensile-strained GaAs/$In_{0.07}Al_{0.93}As$ quantum wells on GaAs substrates.

Sample	Structure
1	100 Å/70 Å/40 Å GaAs wells separated by 200 Å $In_{0.07}Al_{0.93}As$ barriers+500 Å $In_{0.07}Al_{0.93}As$+100 Å GaAs cap
2	100 Å/60 Å GaAs wells separated by a 200 Å $In_{0.07}Al_{0.93}As$ barrier+500 Å $In_{0.07}Al_{0.93}As$+100 Å GaAs cap
3	80 Å GaAs well+500 Å $In_{0.07}Al_{0.93}As$+100 Å GaAs cap
4	25 Å/25 Å GaAs wells separated by a 50 Å $In_{0.07}Al_{0.93}As$ barrier+500 Å $In_{0.07}Al_{0.93}As$+100 Å GaAs cap

perature was 600 and 540 °C for the growth of GaAs and $In_{0.07}Al_{0.93}As$, respectively. A 1000 Å GaAs buffer was first grown on the substrate and it was followed by a 1 μm $In_{0.07}Al_{0.93}As$ layer. GaAs/$In_{0.07}Al_{0.93}As$ quantum wells were then grown on the thick $In_{0.07}Al_{0.93}As$ layer and capped with 100 Å of GaAs. Other sample information is listed in Table I. The PL measurements were excited by the 488 nm line of an Ar^+ laser. The luminescence was dispersed through a double monochromator and detected with a photomultiplier and photon-counting electronics.

RESULTS AND ANALYSIS

The PL spectra are shown in Figs. 1–3. For the multiple-quantum-well samples, the thinnest well is closest to the surface upon which the laser is incident and the thickest well (100 Å) is inner most (see Table I). It is expected that the 100 Å well would experience a lower excitation intensity than the outer wells because of the absorption effect. As shown in Fig. 1, the PL intensity of the 40 Å well is much larger than that of the 100 Å well. The full width at half-maximum (FWHM) of the PL peaks in Figs. 1 and 2 is 8 meV. It can also be seen that a weak-intensity peak also exists 10 meV below the main peak for the 60 Å well. The PL spectrum of a 25 Å quantum well is shown in Fig. 3. On the log scale, it can be seen that there are two peaks of energies 1.743 and 1.787 eV. It is known from PL measurements of a thin GaAs/AlAs quantum well[20,21] that a type-II transition, which arises from the recombination of the electron from AlAs and the hh from GaAs, can be observed in addition to the type-I transition, which arises from the recombination of the electron and hh both in GaAs. A feature of the type-II transition is that its PL peak energy increases as the excitation intensity is increased[22,23] due to the spatially separated electron and hole. As shown in Fig. 4, the PL peak at 1.743 eV moves to higher energy as the excitation intensity increases from 2 to 100 W/cm^2. This indicates that the 1.743 and 1.787 eV peaks are related to the type-II and type-I transitions, respectively.

In order to analyze the PL spectra, the GaAs/$In_{0.07}Al_{0.93}As$ band offset and strain of GaAs have to be known. The strained hh band offset of GaAs/$In_{0.07}Al_{0.93}As$ is determined from the type-I and type-II transitions of the 25 Å quantum well, employing an iterative analysis as described in Ref. 21. In the iterative analysis, the electron and hh confinement energies are calculated from the energy-dependent effective-mass model,[24] which is derived from the four-band $\mathbf{k}\cdot\mathbf{p}$ theory with the inclusion of strain.[25] The material parameters are listed in Table II.[26–31] The intrinsic

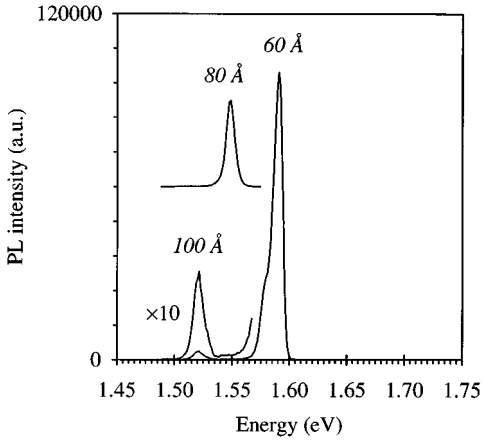

FIG. 2. PL spectrum of 60, 80, and 100 Å GaAs/$In_{0.07}Al_{0.93}As$ quantum wells at 25 K.

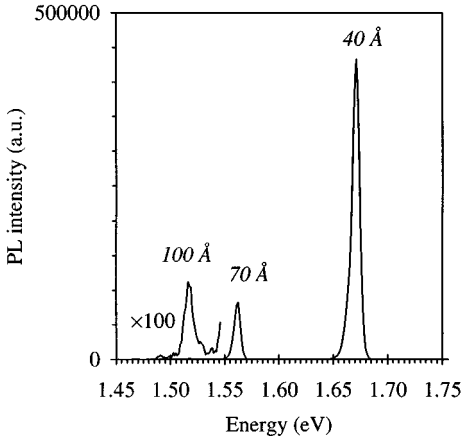

FIG. 1. PL spectrum of 40, 70, and 100 Å GaAs/$In_{0.07}Al_{0.93}As$ quantum wells at 25 K.

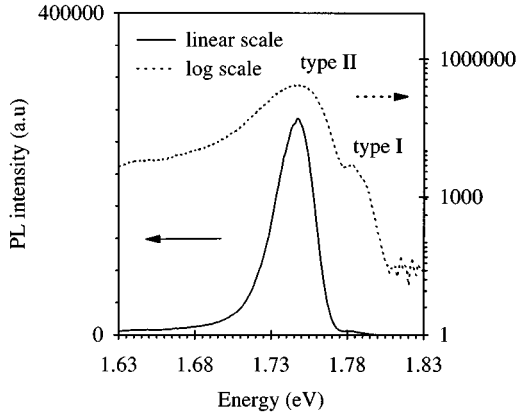

FIG. 3. PL spectrum of a 25 Å GaAs/$In_{0.07}Al_{0.93}As$ quantum well at 29 K.

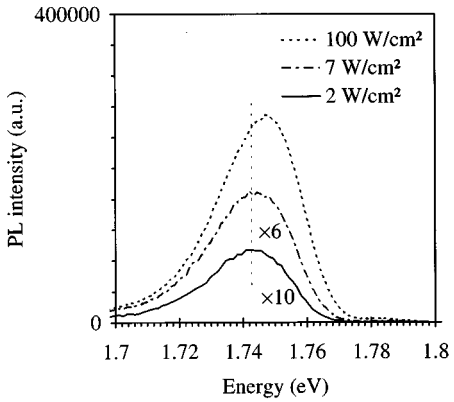

FIG. 4. PL spectrum of a 25 Å GaAs/$In_{0.07}Al_{0.93}As$ quantum well at 29 K under different excitation intensities.

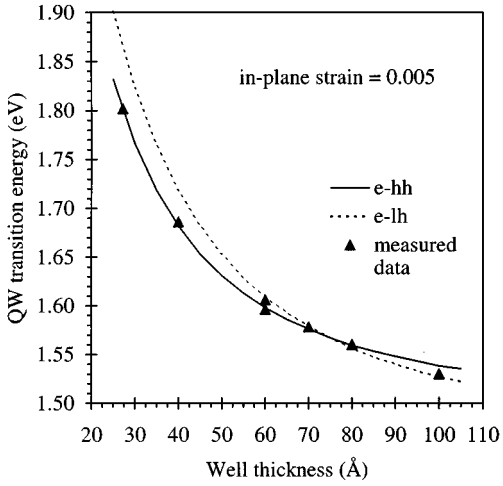

FIG. 5. Comparison of calculated and measured quantum-well transition energies at different well thicknesses for GaAs/$In_{0.07}Al_{0.93}As$. The strain of the GaAs is best fitted with 0.005.

valence-band offset of GaAs/$In_{0.07}Al_{0.93}As$ is obtained from the strained hh band offset and the corresponding strain-induced band-edge shift[25] of GaAs

$$\Delta E_{\mathrm{hh}} = 2a_v\left(1-\frac{c_{12}}{c_{11}}\right)\epsilon + b\left(1+2\frac{c_{12}}{c_{11}}\right)\epsilon, \tag{1}$$

where a_v and b are the valence-band hydrostatic and shear deformation potentials; c_{ij} and ϵ are the elastic constants and the in-plane strain. Using the determined intrinsic valence-band offset of GaAs/$In_{0.07}Al_{0.93}As$, the electron–hh and electron–lh transition energies of strained GaAs/$In_{0.07}Al_{0.93}As$ quantum wells are calculated from the energy-dependent effective-mass model. The result is compared to the measured PL peak energies of various quantum-well thicknesses. It is found that the strain of the GaAs is best fitted with 0.005 as shown in Fig. 5, in which the exciton binding energy of 15 or 10 meV is added to the PL peak energy if the well thickness is smaller or larger than 70 Å, respectively. (The exciton binding energy is estimated from that of GaAs/AlAs quantum wells.)[32] The intrinsic valence-band offset of GaAs/$In_{0.07}Al_{0.93}As$ is found to be 0.56 eV from the iterative analysis. The GaAs well thickness is also determined to be 27.2 Å as a result of the iterative analysis. This value differs from the nominal thickness (25 Å) by ~1 monolayer (2.8 Å). It can be seen in Fig. 5 that the observed PL peak originates from the electron–lh transition at a well thickness of 100 Å and from the electron–hh transition for well thicknesses less than 40 Å. For the PL spectrum of the 60 Å GaAs/$In_{0.07}Al_{0.93}As$ quantum well in Fig. 2, there is another PL peak 10 meV below the main PL peak. The main PL peak is attributed to the e–lh transition and the lower-energy peak to the e–hh transition as indicated in Fig. 5.

The strain of the GaAs was also measured using Raman spectroscopy for the 100 Å/70 Å/40 Å sample. The Raman measurement was performed in the [001] backscattering geometry. The LO phonon frequency of tensile-strained GaAs is 290 cm^{-1} which is compared with that of unstrained GaAs

TABLE II. (a) Elastic constants c_{ij}, conduction-band and valence-band deformation potentials of GaAs. (b) $\mathbf{k}\cdot\mathbf{p}$ parameters[c] (s, γ_i, and E_p), band-gap energies (E_Γ and E_X), and spin–orbit splitting (Δ_{so}) of GaAs and $In_{0.07}Al_{0.93}As$.

a	c_{11} (Mbar)	c_{12} (Mbar)	a_c (eV)	a_v (eV)	b (eV)
	1.18	0.54	−9.3[b]	−1.0[b]	−1.7

b	s	γ_1	γ_2	E_p (eV)	E_Γ[d] (eV)	Δ_{so}[d] (eV)	E_X (eV)
GaAs	−0.940	1.894	−0.482	25.7[e]	1.519	0.341	1.979[d]
$In_{0.07}Al_{0.93}As$[f]	−1.184	0.977	−0.580	23.9	2.895[g]	0.277[g]	2.205[h]

[a]Reference 26.
[b]Reference 27.
[c]s, γ_i, and $E_p(=2mP^2/\hbar^2)$ are related to the band-edge effective masses as described in Ref. 24. The band-edge effective masses (m_e/m, m_{hh}/m, m_{lh}/m, m_{so}/m) are (0.067, 0.35, 0.082, 0.154) (Refs. 26, 28), (0.015, 0.48, 0.20, 0.30) (Ref. 29), and (0.023, 0.35, 0.026, 0.09) (Refs. 28, 30) for GaAs, AlAs, and InAs, respectively, where m is the free electron mass.
[d]Reference 28.
[e]Reference 31.
[f]s, γ_i, and E_p of $In_{0.07}Al_{0.93}As$ are linearly interpolated from those of AlAs and InAs.
[g]Quadratic interpolation from those of AlAs and InAs as in Ref. 26.
[h]Measured from low-temperature (25 K) PL.

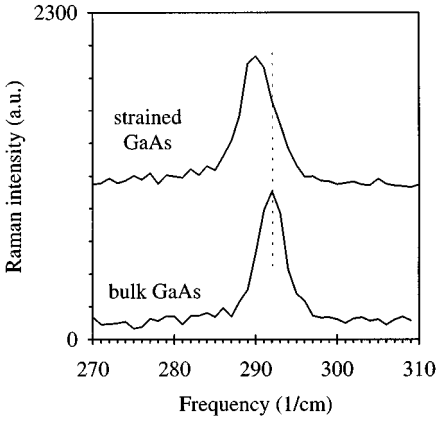

FIG. 6. Raman spectra of tensile-strained GaAs/$In_{0.07}Al_{0.93}As$ and unstrained GaAs.

(292 cm^{-1}) in Fig. 6. Because of the tensile strain, the strained LO phonon frequency decreases as expected from the elastic model.[33] The strain-induced shift of the GaAs LO phonon frequency is[34,35]

$$\Delta\omega_{\mathrm{LO}}=\frac{\epsilon}{\omega_{\mathrm{LO}}}\left(p\,\frac{S_{12}}{S_{11}+S_{12}}+q\right)=-485\epsilon, \tag{2}$$

where ω_{LO} and ϵ are the unstrained LO phonon frequency and the strain; $p(q)$ and S_{ij} are the LO phonon deformation potentials and the elastic compliance. The strain of the GaAs is determined to be 0.004 which agrees with the value from PL measurements.

CONCLUSION

$GaAs/In_{0.07}Al_{0.93}As$ tensile-strained quantum wells were grown on [001] GaAs substrates buffered with a 1-μm-thick $In_{0.07}Al_{0.93}As$ relaxed layer using molecular-beam epitaxy. The strain of the GaAs from Raman and PL measurements is 0.004 and 0.005, respectively. From the $\mathbf{k}\cdot\mathbf{p}$ theory and PL measurements, it is demonstrated that the PL peak originates from the $e-$lh transition for the 100 Å well and from the $e-$hh transition if the well thickness is less than 40 Å. The introduction of tensile strain into the GaAs quantum well through a thick Al-rich $In_xAl_{1-x}As$ buffer can be useful to engineer the relative energy position of the hh and the lh for the GaAs quantum well. This feature is necessary for the in-plane polarization-insensitive electroabsorption or photodetection devices utilizing GaAs quantum wells.

ACKNOWLEDGMENTS

This work was supported by the NSF under Grant Nos. DMR-9224877 (C.N.Y. and L.E.M.) and DMR-9208381 (T.D.-R. and L.J.B.).

[1] D. F. Welch, W. Streifer, C. F. Schaus, S. Sun, and P. L. Gourley, Appl. Phys. Lett. **56**, 10 (1990).
[2] P. J. A. Thijs, L. F. Tiemeijer, P. I. Kuindersama, J. J. M. Binsma, and T. Van Dongen, IEEE J. Quantum Electron. **27**, 1426 (1991).
[3] E. Yablonovitch and E. O. Kane, J. Lightwave Technol. **LT-4**, 504 (1986).
[4] M. P. Huang and Y. C. Chang, J. Appl. Phys. **65**, 3098 (1989).
[5] S. L. Chuang, Phys. Rev. B **43**, 9649 (1991).
[6] T. Higashi, T. Ikeda, S. Ogita, K. Morito, and H. Soda, IEEE J. Quantum Electron. **31**, 286 (1995).
[7] M. P. C. M. Krijn, G. W. 't Hooft, M. J. B. Boermans, P. J. A. Thijs, T. Van Dongen, J. J. M. Binsma, L. F. Tiemeijer, and C. J. Van der Poel, Appl. Phys. Lett. **61**, 1772 (1992).
[8] T. Yamamoto, H. Nobuhara, K. Tanaka, T. Inoue, T. Fujii, and K. Wakao, Jpn. J. Appl. Phys. **33**, 6199 (1994).
[9] C.-S. Chang and S. L. Chuang, Appl. Phys. Lett. **66**, 795 (1995).
[10] M. Yamanishi and I. Suemune, Jpn. J. Appl. Phys. **23**, L35 (1984).
[11] J. S. Wiener, D. S. Chemla, D. A. B. Miller, H. A. Haus, A. C. Gossard, W. Wiegmann, and C. A. Burrus, Appl. Phys. Lett. **47**, 664 (1985).
[12] K. Fujiwara, N. Tsukada, T. Nakayama, and T. Nishino, Appl. Phys. Lett. **51**, 1717 (1987).
[13] S. Chelles, R. Ferreira, P. Voisin, A. Ougazzaden, M. Allovon, and A. Carenco, Appl. Phys. Lett. **64**, 3530 (1994).
[14] T. Aizawa, K. G. Ravikumar, S. Suzaki, T. Watanabe, and R. Yamauchi, IEEE J. Quantum Electron. **30**, 585 (1994).
[15] D. P. Bour, K. J. Beernink, D. W. Treat, T. L. Paoli, and R. L. Thornton, IEEE J. Quantum Electron. **30**, 2738 (1994).
[16] D. P. Bour, R. S. Geels, D. W. Treat, T. L. Paoli, F. Ponce, R. L. Thornton, B. S. Krusor, R. D. Bringan, and D. F. Welch, IEEE J. Quantum Electron. **30**, 593 (1994).
[17] M. Watanabe, H. Matsuura, and N. Shimada, J. Appl. Phys. **76**, 7942 (1994).
[18] H. Kato, N. Iguchi, S. Chika, M. Nakayama, and N. Sano, Appl. Phys. Lett. **59**, 588 (1986).
[19] Y.-C. Chan, T. Morimoto, and K. Tada, Jpn. J. Appl. Phys. **32**, L1596 (1993).
[20] P. Dawson, K. J. Moore, and C. T. Foxon, Proc. SPIE **792**, 208 (1987).
[21] C. N. Yeh, L. E. McNeil, L. J. Blue, and T. Daniels-Race, J. Appl. Phys. **75**, 4541 (1995).
[22] J. Chen, D. Patel, J. R. Sites, I. L. Spain, M. J. Hafich, and G. Y. Robinson, Solid State Commun. **75**, 693 (1990).
[23] R. Teissier, R. Planel, and F. Mollot, Appl. Phys. Lett. **60**, 2663 (1992).
[24] M. F. H. Schuurmans and G. W. 't Hooft, Phys. Rev. B **31**, 8041 (1985).
[25] F. H. Pollak, in *Semiconductors and Semimetals*, edited by T. P. Pearsall (Academic, New York, 1991), Vol. 32, Chap. 1.
[26] M. P. C. M. Krijn, Semicond. Sci. Technol. **6**, 27 (1991).
[27] D. D. Nolte, W. Walukiewicz, and E. E. Haller, Phys. Rev. Lett. **59**, 501 (1987).
[28] O. Madelung, *Intrinsic Properties of Group IV Elements and III-V Compounds* (Springer, New York, 1987).
[29] E. Hess, H. Neumann, and I. Topol, Phys. Status Solidi B **55**, 187 (1973).
[30] P. Lawaetz, Phys. Rev. B **4**, 3640 (1971).
[31] L. G. Shantharama, A. R. Adams, C. N. Ahmad, and R. J. Nicholas, J. Phys. C Solid State Phys. **17**, 4429 (1984).
[32] M. Gurioli, J. Martinez-Psator, M. Colocci, A. Basacchi, S. Franchi, and L. C. Andreani, Phys. Rev. B **47**, 15755 (1993).
[33] E. Anastassakis, in *Light Scattering in Semiconductor Structures and Superlattices*, edited by D. J. Lockwood and J. F. Young (Plenum, New York, 1991), p. 173.
[34] G. Attolini, L. Francesio, P. Franzosi, C. Pelosi, S. Gennari, and P. P. Lotici, J. Appl. Phys. **75**, 4156 (1994).
[35] G. Landa, R. Carles, C. Fontaine, E. Bedel, and A. Munoz-Yague, J. Appl. Phys. **66**, 196 (1989).